12th International Workshop on Wave Hindcasting and Forecasting, Kohala Coast, Hawai'i, HI, 2011.

QUASI-STATIONARY WAVEWATCH III® FOR THE NEARSHORE [1]

André J. van der Westhuysen[2,3] and Hendrik L. Tolman[4]

Abstract

With the increased frequency and severity of hurricane and inundation events, it has become important to extend the field of application of WAVEWATCH III® to the nearshore. Since this model is based on the hyperbolic form of the action balance equation, CFL restrictions apply to the choice of the propagation time step, rendering nearshore simulation with high spatial resolution computationally expensive. In the present study, a quasi-stationary version of WAVEWATCH III® is developed. Advantage is taken of the fact that quasi-stationary conditions can develop over a domain of limited spatial extent during a model input/output interval. Under these conditions, the solution can be accelerated by the ratio of this interval to the residence time of energy inside the domain. Within each input/output interval, time stepping is carried out up to the residence time, followed by a discontinuous jump to the beginning of the next input/output interval. Boundary conditions from the offshore domain are nonstationary, but brought forward in time by the difference between the input/output interval and the residence time to ensure proper phasing. The resulting quasi-stationary model is evaluated for idealized swell propagation and a field case of a highly nonstationary hurricane event. Computational savings of up to 50% relative to the default nonstationary model are found, depending on the wave conditions and domain size, in combination with local errors in significant wave height and mean period of less than 5% and 2%, respectively. The model operation investigated here is limited to the one-way nesting (ww3_shel) mode, but the method is extendable to the two-way nesting (ww3_multi) mode.

1 INTRODUCTION

WAVEWATCH III®, hereafter WW3, is a leading spectral wind wave model for the computation of wave fields on oceanic scale. In recent years, a need has arisen to extend the field of operation of this model towards the nearshore. To this end, parametrizations of nearshore physical processes such as depth-induced breaking have been included (Tolman, 2009). However, in addition, if explicit propagation schemes are applied, the numerical approach of the model needs to be adapted in order to deal efficiently with the smaller CFL time steps for geographical propagation imposed by the increased spatial resolution required to resolve the nearshore processes (e.g. Monbaliu et al., 2000; Brown and Wolf, 2009).

In these coastal domains, the residence time t_s of wave energy is typically shorter than the time scale of change of the boundary conditions and forcing. Hence, wave fields often become approximately (quasi) stationary over domains of limited extent along the coastline on the time scales that output is required, denoted by Δt_s. This premise has been the motivation for developing fully stationary nearshore spectral wave models such as HISWA (Holthuijsen et al., 1989), STWAVE (Davis, 1992; Smith et al., 1999) and SWAN (Booij et al., 1999) in the past. The latter model uses an implicit elliptical scheme (a four-sweep Gauss-Seidel method) for geographical propagation, and was later extended for nonstationary operation in the offshore. Here we present an approach for adapting WW3 for nearshore application, using hyperbolic equations (explicit propagation schemes), by taking advantage of this quasi-stationarity of the nearshore wave fields. The intended application of this quasi-stationary model version is high-resolution coastal nesting in larger domain offshore grids, which are run in conventional nonstationary mode. We will introduce the concept of "time stretching" for these nearshore applications,

[1] MMAB contribution Nr. 295

[2] E-mail:Andre.VanDerWesthuysen@NOAA.gov
[3] UCAR Visiting Scientist at NOAA/NWS/National Centers for Environmental Prediction.
[4] NOAA/NWS/National Centers for Environmental Prediction, 5200 Auth Road, Camp Springs, MD 20746, USA.

in which the time stepping through physical time is accelerated by the ratio of the input/output interval Δt_s to the residence time t_s. The solution obtained can be distributed over the output increment in a pre-determined fashion (linear, incremental, etc.). The ratio of t_s to Δt_s therefore represents the reduced computational time relative to the non-stationary model achievable with this approach.

The aim of this study is to develop the above-mentioned quasi-stationary solution method for WW3 and to evaluate the resulting model for idealized cases and field cases in the nearshore.

The achieve this aim, first the concepts of time stretching and quasi-stationary model operation are presented in Section 2. In Section 3 the operation of this quasi-stationary model is illustrated for an idealized case of wave propagation, and subsequently applied to the highly nonstationary case of Hurricane Gustav which made landfall at the Louisiana coast, USA, in August-September 2008. Section 4 presents a discussion on the results and Section 5 closes with conclusions. The implementation studied here is limited to the one-way nesting (ww3_shel) mode of WW3. However, this method can be extended to the multigrid (ww3_multi) mode of WW3, as will be discussed in Section 4.

2 APPROACH

In this section, the basic approach of the quasi-stationary version of WW3 is presented, including the related issues of computing the quasi-stationary time scale t_s and the implications of the CFL constraint on simulation times in the nearshore.

2.a Basic approach

WW3 models the evolution of the wind wave action spectrum $N(k,\theta;\vec{x},t)$, where $N(k,\theta;\vec{x},t) = F(k,\theta;\vec{x},t)/\sigma$ with F the variance density spectrum and σ the radian frequency, using the action balance equation (e.g. Hasselmann 1960):

$$\frac{\partial N(k,\theta;\vec{x},t)}{\partial t} + \nabla\cdot\vec{c}N(k,\theta;\vec{x},t) = \frac{S(k,\theta;\vec{x},t)}{\sigma} \quad , \quad (1)$$

where k and θ are the wavenumber and direction, respectively, $\vec{x}$ and t are geographical space and time, respectively, $\vec{c}$ represents the characteristic velocities in geographical and spectral space (including the possible influence of currents) and S represents the total of all sources and sinks of wave energy. Equation (1) is typically applied in WW3 in a hyperbolic form.

In the nearshore, the time required for reaching stationarity (the residence time) is often shorter than the time scale of change of the boundary conditions and forcing, so that the solution becomes quasi-stationary. A number of time scales are defined. The first is the time scale for reaching stationarity t_s (residence time), defined as

$$t_s = \alpha t_t \quad (2)$$

where t_t is the transient time of dominant wave information with a given propagation speed through a given grid, and α is a factor somewhat greater than 1. Quasi-stationary solutions can be expected to be valid at the end of each model input/output interval Δt_s if

$$t_s << \Delta t_s \ . \quad (3)$$

These two time scales can be used to express the possible increase in computational speed γ as:

$$\gamma = \Delta t_s / t_s \quad , \quad (4)$$

where γ will be greater than 1 if (3) is satisfied. Conceptually, the proposed quasi-stationary model operation can be viewed as follows: for each global time step Δt_n on the nearshore grid, the increments in action density from (1) are computed as

$$\Delta N(k,\theta;\vec{x},t) = \Delta t_n \left[\frac{S(k,\theta;\vec{x},t)}{\sigma} - \nabla\cdot\vec{c}N(k,\theta;\vec{x},t) \right] \ , \quad (5)$$

but accelerated by the factor γ in physical time:

$$t_i = t_{i-1} + \gamma \Delta t_n \ . \quad (6)$$

The global time step Δt_n would still satisfy stability requirements in the nearshore, but the effective time step of integration would be greater. The expression (6) represents a linear time stretching and the gain in computational speed.

There are various approaches to implementing (6), taking into account also the treatment of boundary conditions, which the nearshore quasi-stationary simulation will typically receive from a larger domain grid. Here we propose a method of discontinuous time stepping combined with discontinuous, nonstationary boundary conditions. In this approach, the quasi-stationary calculation is carried out with the global time step Δt_n up to the residence time t_s, after which the global time counter t_i is discontinuously incremented up to the end of the input/output interval Δt_s:

$$t_i = t_0 + \left[i + (n_m - n_i) \lfloor \frac{i}{n_i} \rfloor \right] \Delta t_n, \quad i = 1..N, \quad (7)$$

where t_0 is the time at the beginning of the computation, t_i are the points in time at which computations are carried out, $n_m = \Delta t_s / \Delta t_n$ and $n_i = t_s / \Delta t_n$. The residence time t_s is dynamically computed using (10) within the current input/output interval Δt_s, discussed below, and then applied as a fixed model parameter in the subsequent Δt_s interval. The time varying boundary condition from the larger domain simulation is applied continuously over the interval Δt_s, sampled at each t_i. Hence the boundary condition for the nested domain becomes:

$$\psi_i = \psi(t_i) \quad , \quad (8)$$

with $\psi(t)$ the continuous nonstationary boundary condition from the larger domain. In order to avoid the phase lag induced by the discontinuous time stepping in (7), the updating of the boundary conditions is phase-shifted forward by $(\Delta t_s - t_s)$ during each output interval Δt_s. This is achieved with the following boundary value specification:

$$\psi_i = \psi(t_i + (\Delta t_s - t_s)) \quad . \quad (9)$$

In this way, the nonstationary boundary condition reaches the value of $\psi(\Delta t_s)$ at the end of the residence time interval t_s, as required, before skipping discontinuously to the next output interval Δt_s.

2.b Computation of t_s and Δt_s

The residence time t_s is a function of a number of variables, including: (a) the dimensions of the nearshore grid, (b) the characteristic wave energy propagation speed and direction, and (c) the time scale of the environmental forcings (e.g. wind and water level). The largest possible value of t_s is found by considering the diagonal of the (rectangular) domain, and the highest spectral wavenumber in the discretized spectrum. This would, however, yield very large values for t_s, unnecessarily reducing γ.

An alternative is to dynamically compute t_s on the basis of the dominant wave condition. This may be done on the basis of the time scales of change of the boundary conditions, but this may neglect important wind sea components generated inside domain on the time scale of (c). Hence, the residence time scale is computed from the evolving solution throughout the simulation. It is computed on the basis of $c_{g,\tilde{T}_{\mathrm{m01}}}$, the propagation speed of wave energy associated with the spatial mean period $\tilde{T}_{\mathrm{m01}}$, and X, the propagation distance over the domain using the domain-averaged mean wave direction, and assuming the domain to be rectangular and without landmass. The mean period $\tilde{T}_{\mathrm{m01}}$ is used, and not, for example, the peak period, in order to weight the result towards slower-moving components in the spectral tail. The resulting residence time parameter is:

$$t_s = \alpha t_t = \alpha \frac{X}{c_{g,\tilde{T}_{\mathrm{m01}}}} \quad . \quad (10)$$

In the simulations presented here, the factor α was set to 1.2 in order to ensure that most of the energetic components have traveled across the domain.

The input/output time step Δt_s is set by the user, based on the available frequency of inputs and the desired frequency of outputs. It is assumed that Δt_s will be chosen such that the boundary conditions and forcing do not change significantly over its duration.

2.c CFL constraints

Having defined the general principle of the quasi-stationary operation and the residence time scale t_s, we subsequently estimate the expected total impact of quasi-stationary operation on the simulation times in the nearshore. In general, the gain in computational speed γ due to stationarity and the time compression method is offset by the fact that the CFL time step in the nearshore $\Delta t_{\mathrm{CFL,n}}$ will typically be much smaller than that in the offshore

$\Delta t_{\mathrm{CFL,os}}$. The CFL criterion for spatial propagation using the current hyperbolic equations of WW3 is given by (Tolman, 2009):

$$\mathrm{CFL} = \frac{\dot{x}\Delta t}{\Delta x} < 1 \quad , \tag{11}$$

where Δt represents the integration time step, Δx a spatial step and $\dot{x}$ the propagation velocity of wave energy ($= \vec{c}_g + \vec{U}$). If we subsequently require (a) an equal CFL number in the offshore and nearshore, (b) assume that the wave energy propagation speeds are similar in both domains, and (c) assume that the global time steps Δt_n and Δt_{os} are directly related to the CFL time steps for geographical propagation, then the nearshore time step will be given by:

$$\Delta t_n = \frac{\Delta x_n}{\Delta x_{os}} \Delta t_{os} = \beta \Delta t_{os} \ , \tag{12}$$

where Δx_n and Δx_{os} are the nearshore and offshore spatial discretization steps and $0 < \beta < 1$ their ratio (for $\Delta x_n < \Delta x_{os}$). Hence, substituting (12) in (6), the effective change in the time stepping relative to that in the offshore is given conceptually by

$$t_i = t_{i-1} + \gamma\beta\Delta t_{os} \ . \tag{13}$$

Given an equal number of geographical grid points in both domains, it follows from (13) that equal or greater computational speed in the nearshore will be realized for $\gamma > \beta^{-1}$. Simple arithmetic examples show that the reduction in speed due to the reduced spatial steps β typically outweighs the gain due to quasi-stationarity γ in (13). This implies that nearshore high-resolution modeling with hyperbolic equations will likely remain more expensive than offshore applications of similar total grid node size. We return to this issue in Section 4.

3 SIMULATIONS

In this section, the quasi-stationary version of WW3 presented above is evaluated by means of numerical simulation. First the model is applied to a simple wave propagation case over an idealized deep water basin, and subsequently to a field case of Hurricane Gustav over nearshore Louisiana. As discussed in Section 1, all simulations presented here are based on the one-way nesting (ww3_shel) version of WW3.

3.a Idealized deep water basin with nesting

The performance of the proposed quasi-stationary model is first evaluated for an idealized model of wave propagation over a larger grid into a nested grid (one-way nesting), in deep water. Figure 1 shows the model grid setup applied for this purpose. It features a deep water coarse grid (50 x 250 km), which is run in conventional, fully-nonstationary mode. A near-monochromatic, long-crested wave field ($H_{\mathrm{m0}} = 0.1$ m, $f_{\mathrm{p}} = 0.33$ Hz, Std. dev. = 0.01 Hz, Dir = 270°N) is imposed on the coarse grid. In the absence of an option for time-varying boundary condition specification in WW3, this wave condition is imposed with a normal distribution of wave energy in space ($\tilde{X}$ = 10 km, Std. dev. = 7.5 km), using a Type 1 initial field. This creates a sinusoidal pulse of wave energy in time that propagates towards the nested grid. Boundary conditions for the nested grid are output every 3600 s, which is also the output interval Δt_s of the system.

The nested grid subsequently receives the boundary conditions and performs a quasi-stationary run. On this grid, the global time step is $\Delta t_{\mathrm{n}} = 150$ s, the time step for propagation in geographical and spectral spaces are $\Delta t_{\mathrm{CFL,x-y}} = 150$ s and $\Delta t_{\mathrm{CFL,k-}\theta} = 150$ s respectively, and the minimum source term integration step is $\Delta t_{\mathrm{sources,min}} = 15$ s. The results of the quasi-stationary model and the default non-stationary version will be considered at Stations 1 and 2, at X = 45.5 km and 49.5 km respectively (Figure 1).

Figures 2 and 3 show the results of the quasi-stationary model, and compare them to the results for a default, fully nonstationary simulation. Figure 2(a) shows the evolution of H_{m0} at each global time step t_i for both the default and quasi-stationary runs. Panel (b) shows the variation of the residence time scale t_s. The latter starts at the user-specified default value (3600 s). After the first output interval Δt_s (vertical lines), t_s shifts to a computed value of about 2500 s, corresponding to the residence time of the lower-frequency components in the narrow frequency distribution. It subsequently increases gradually to $t_s \approx 2800$ s as higher frequencies reach the nested domain. Also included in panel (b) is the duration of Δt_s (= 3600 s here). For all $t_s < \Delta t_s$, a quasi-stationary simulation is possible over the interval Δt_s.

From Figure 2(b) it can be seen that for the first two output intervals, $t_s \not< \Delta t_s$ at the end of the previ-

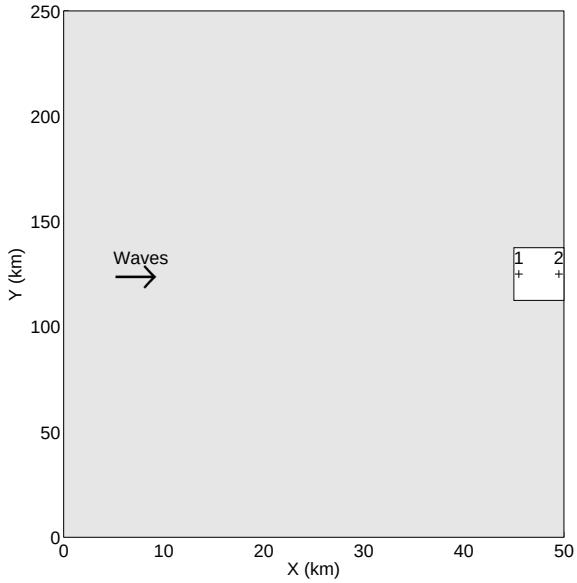

Fig. 1: Model setup for the wave propagation test. Overall model grid (50 x 250 km) in gray and nested grid (5 x 25 km) in white. Wave direction indicated by the arrow, and output stations in the nested grid labeled as 1 and 2. Note the different scales on the x and y axes.

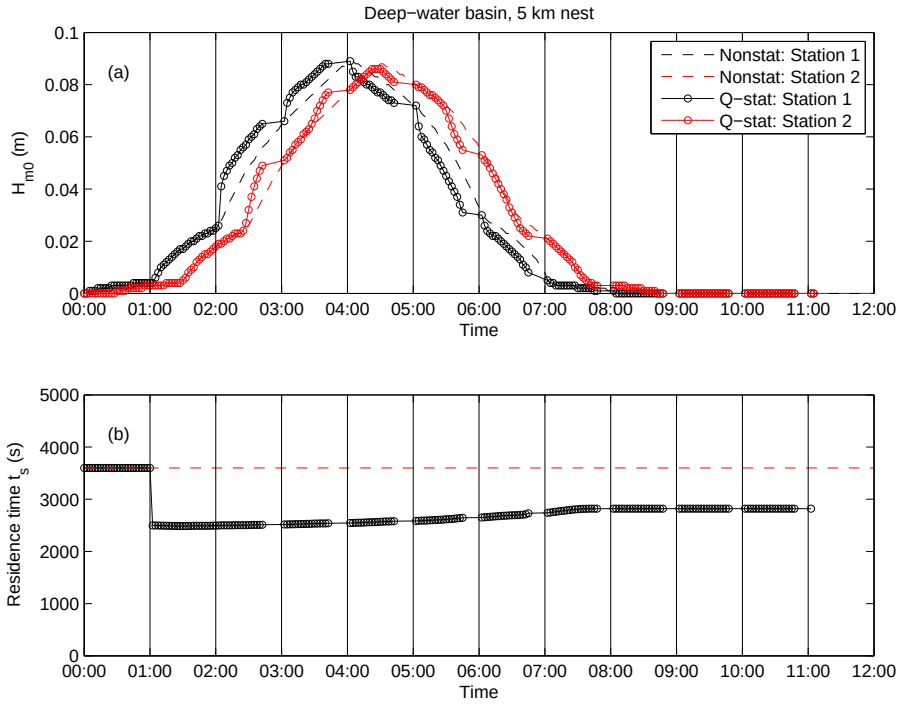

Fig. 2: Results of the quasi-stationary and default nonstationary models for the wave propagation test (nested 5 km grid). Panel (a): evolution of H_{m0} at Stations 1 and 2. Circles indicate the time steps Δt_n. Panel (b): evolution of the residence time scale t_s. Dashed line shows duration of output interval Δt_s (here 3600 s). Output interval Δt_s also indicated in time as vertical lines.

ous interval (or start of the simulation), and hence a fully nonstationary computation is made. From the third Δt_s interval onwards, $t_s < \Delta t_s$, and hence a quasi-stationary computation is carried out. Figure 2(a) shows how in this third time interval the solution at the upwave Station 1 is brought forward in time by $(\Delta t_s - t_s)$ relative to the boundary condition time series from the coarse grid. The boundary condition value of $\psi(\Delta t_s)$ is reached at the residence time t_s, after which the quasi-stationary computation is suspended until the start of the next output interval Δt_s. The effect of this 'speeding-up' of the boundary input is that the quasi-stationary solution at Station 2 now shows increased growth and decay rates within each t_s interval. As a result, after t_s, the solution is at the level that the default nonstationary solution reaches at Δt_s. The solution at the end of the residence time t_s is transferred to the beginning of the next output interval Δt_s. The result is that, considering the values at the output intervals Δt_s, the solutions at both Stations 1 (upwave) and 2 (downwave) follow those of the default model (Figure 3). Note that the solution at Station 2 of the default model differs from that of the boundary only due to aliasing effects in the sampling of points along the curve (see Figure 2).

It can thus be seen that the application of the nonstationary, phase-shifted boundary conditions in this approach avoids the spurious phase shift associated with stationary elliptical solutions.

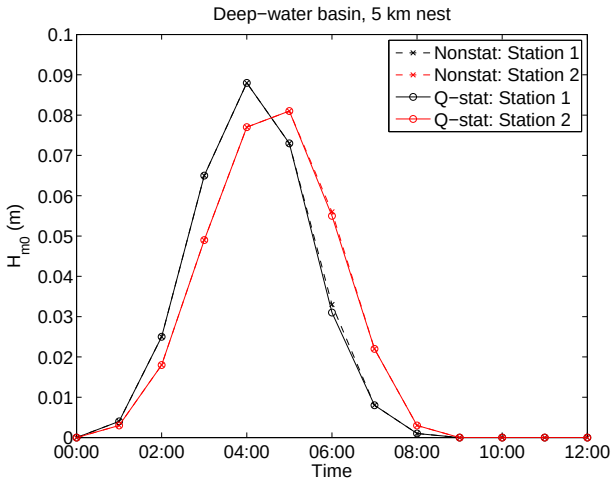

Fig. 3: Time series of H_{m0} output of default and quasi-stationary runs at Stations 1 and 2 in wave propagation test.

3.b Field case: Hurricane Gustav

The quasi-stationary WW3 model is next evaluated for a field case featuring nearshore application in a highly nonstationary hurricane case. The case considered is that of Hurricane Gustav, which occurred in August–September 2008. After passing over the Caribbean and the Gulf of Mexico, Gustav made its final landfall near the town of Cocodrie, LA, around 15:00 UTC on September 1, with maximum winds near 90 kt (Category 2, National Hurricane Center 2008).

This case is modeled using a series of five regular, one-way nested grids, based on data from Chen et al. (2010). The set starts with an outer grid, including the Gulf of Mexico and the Caribbean Sea, and ends with a small nearshore grid that includes the nearshore NDBC buoy 42007 (just outside of the Chandeleur islands), being the closest buoy to the point of landfall (Grids 1–5, Table 1). The spatial resolution in these grids varies from 12 arc min (Grid 1) to a high resolution of 100 m on the small nearshore domain (Grid 5), with a 10x10 km extent. Figures 4 and 5 show Grids 3–5 closest to the coast. Included in Figure 4 is the best track of Gustav, showing the landfall at Cocodrie. Also shown in Figures 4 and 5 is the location of NDBC buoy 42007 (refer Table 2). The wind fields applied over these domains have been produced by a parametric analytic wind model for asymmetric hurricanes (Hu et al., 2010), merged with large scale background wind fields from GFS. In addition, the simulations include time-varying water level fields, computed using the storm surge model ADCIRC (Luettich and Westerink 2004; Westerink et al. 2008).

Regarding the wave model settings, the spectral resolution consists of 29 logarithmically distributed frequencies (starting at 0.035 Hz) and 24 discrete directions. The present default set of source terms is applied, namely wind input and whitecapping according to Tolman and Chalikov (1996), and the default expressions for quadruplet interaction, bottom friction and depth-induced breaking. Wave propagation in geographical space and depth refraction are activated, but not current-induced Doppler shifting and refraction. The frequency for model inputs (winds and water level) and outputs was set at Δt_s = 3600 s. Table 1 presents time steps applied. The time step Δt_n on Grid 5 is 240 times smaller than that of the offshore Grid 1, reflecting the ratio of the grid cell sizes in the light of CFL restrictions. The model was run in default nonstationary mode on all

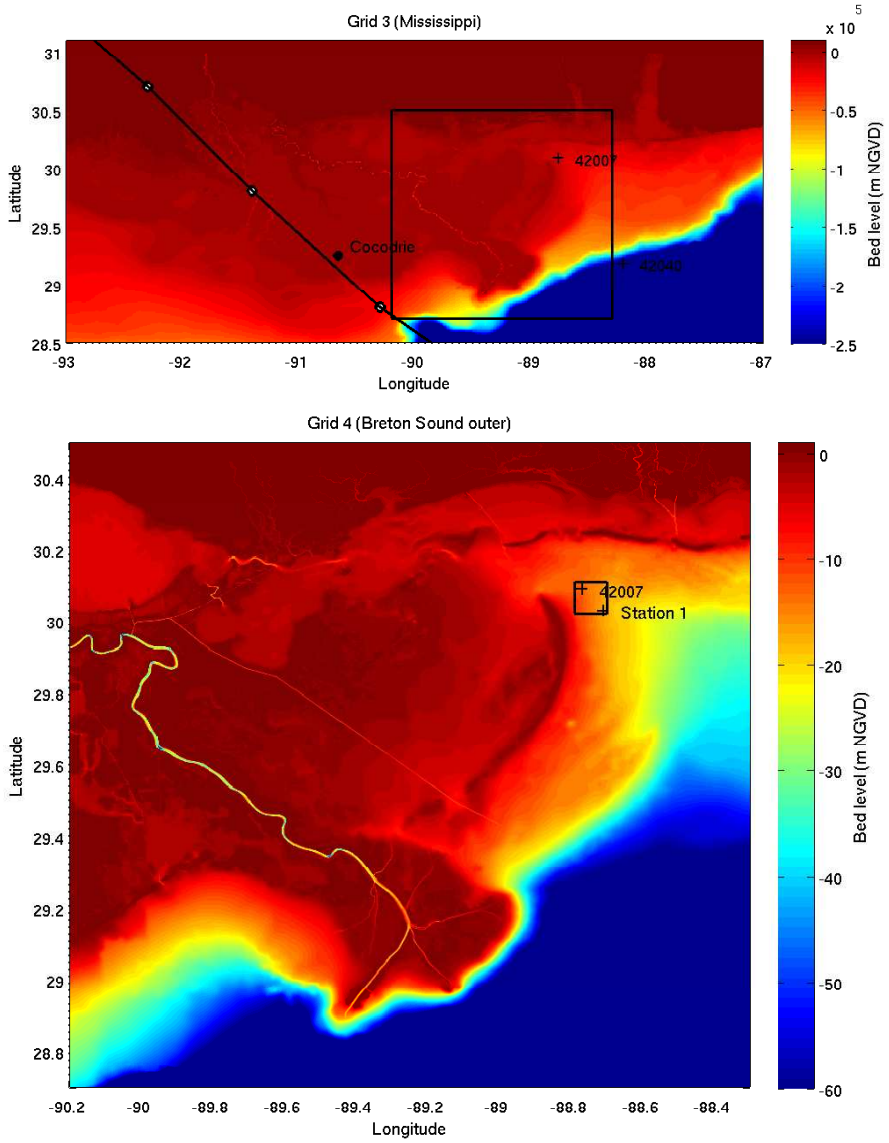

Fig. 4: Bathymetry of Grid 3 (Mississippi Delta, 1 km, top, with nest of Grid 4) and Grid 4 (Breton Sound outer, 250 m, bottom, with nest of Grid 5). Curve indicates the best track for Hurricane Gustav.

Table 1: Cell sizes and time steps for the various grids in the Hurricane Gustav simulation.

Grid	Δx	Δt_{n} (s)	$\Delta t_{\mathrm{CFL,x-y}}$ (s)	$\Delta t_{\mathrm{CFL,k-}\theta}$ (s)	$\Delta t_{\mathrm{sources,min}}$ (s)
1	12 arc-min	1200.	700.	600.	5.
2	3 arc-min	300.	180.	150.	5.
3	1 km	60.	35.	30.	5.
4	250 m	15.	9.	7.5	1.
5	100 m	5.	3.6	2.5	1.

five model grids, and repeated on Grid 5 using the quasi-stationary mode. The total run time for the nonstationary model on Grid 5 was 67 min, using 16, 32-way nodes (= 512 cores) on an IBM Power6 Cluster, each with a 4.7 GHz processor, run using MPI parallel directives.

Table 2: Coordinates of output stations in the Hurricane Gustav simulation.

Station	Long. (degr.)	Lat. (degr.)
42007	-88.77	30.09
'Station 1'	-88.71	30.03

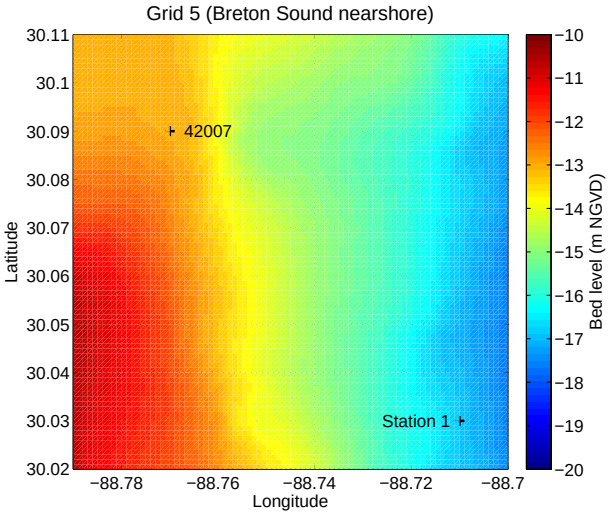

Fig. 5: Bathymetry of Grid 5 (Breton Sound nearshore, 10x10 km, 100 m), including locations of NDBC buoy 42007 and upwave output point Station 1.

Figure 6 compares the behavior of the quasi-stationary and default nonstationary model modes at Station 1 and buoy 42007 on the nearshore Grid 5. Panels (b) and (d) of this figure show the variation of the residence time t_s, which reflects the variation in the mean wave period between $T_{m01} = 4$–11 s (not shown). At the beginning of the simulation, before sufficient amounts of wave energy have entered the initially calm domain of Grid 5, high values of t_s are found (not shown). As the hurricane nears landfall, t_s steadily reduces so that for a 36 hour period at the peak of the event at buoy 42007, t_s falls to about 50% of the output interval $\Delta t_s = 3600$ s (dashed red line). After the peak, t_s increases again to above Δt_s. Hence it can be seen that, despite the high nonstationarity of the conditions, quasi-stationary operation is possible at the event peak due to the fact that the residence time of the longer waves falls below that of the chosen output interval. However, since this constitutes a relatively short period of the total simulation time, the total saving in run time remains limited: the quasi-stationary run time comes to 61 min, or 91% of that of the default nonstationary simulation. Options for further optimization are discussed in Section 4 below.

Panels (a) and (c) of this figure show the hourly H_{m0} output of the default nonstationary model at the output point near the upwave boundary of Grid 5 (Station 1), and at buoy 42007 near the downwave grid edge. They show the typical signature of a hurricane event, featuring initially low values of wave height sharply increasing and subsequently decreasing as the hurricane passes. Superimposed on these are the H_{m0} output of the quasi-stationary model after each time step Δt_n. As before, the output intervals are indicated by vertical lines, for reference. Figure 6(a) shows a good agreement between the results of the quasi-stationary and the default nonstationary results throughout the hurricane passing. Figure 6(c) presents a detailed view of the comparison for the 36 hours leading up to, and including the peak of the event at buoy 42007 (landfall). The quasi-stationary mode, active here, displays similar behaviour to that shown in Figure 2 above. At both the upwave and the downwave output locations, the solutions at the start and end of the output interval match that of the default nonstationary run closely.

Figure 7 compares the H_{m0} and T_{m01} results of the quasi-stationary and default nonstationary models at only the output intervals Δt_s. The results of the quasi-stationary version, active over the 36 h period centered on 09/01, can be seen to agree well with those of the default nonstationary model. Panels (c) and (f) show that the maximum errors in H_{m0} and T_{m01} with respect to the nonstationary model result are 1% and 0.5% respectively, which are considered acceptably low.

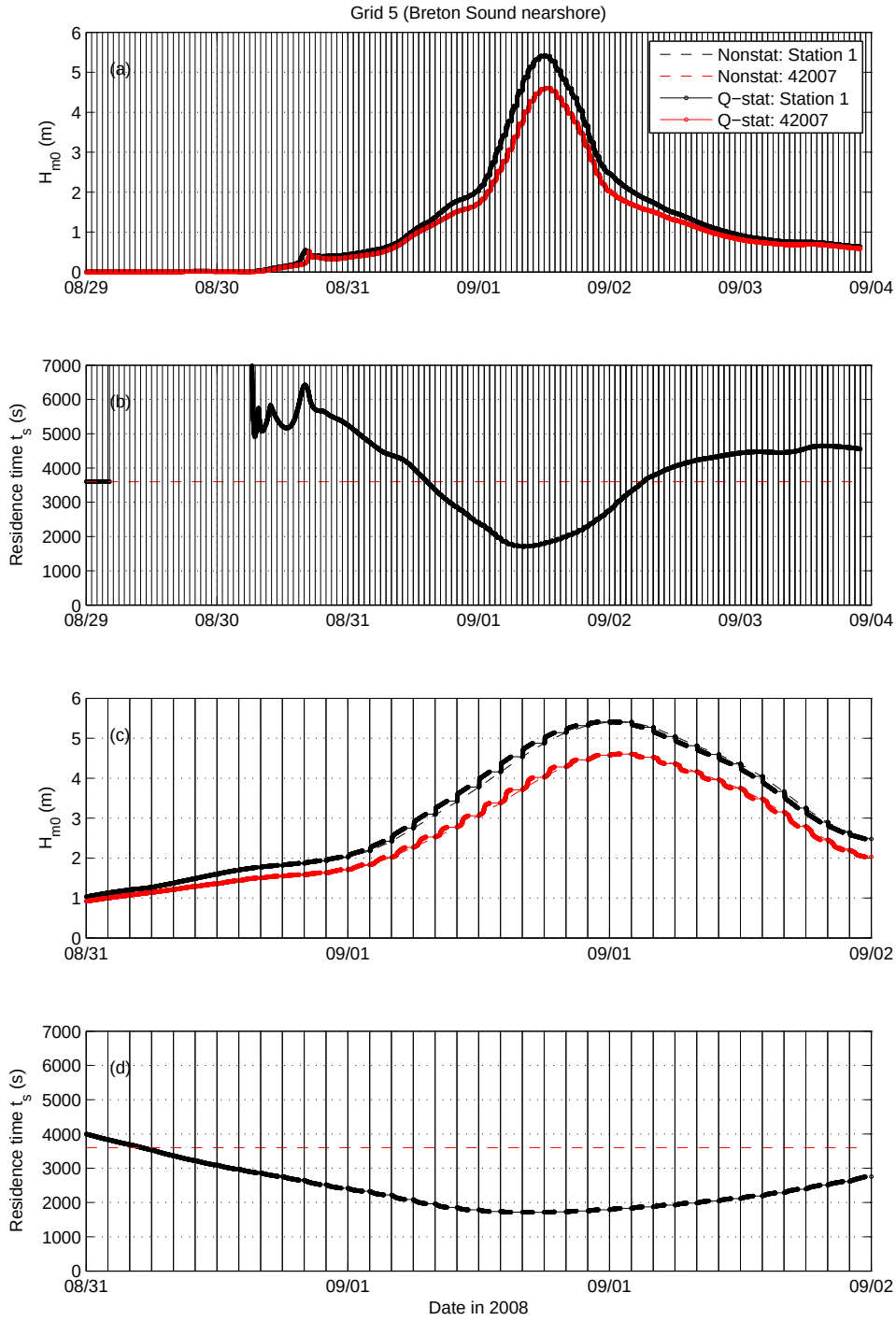

Fig. 6: Results of the quasi-stationary and default nonstationary models for Hurricane Gustav case on Grid 5 (Breton sound nearshore). Panel (a): evolution of H_{m0} at two stations. Circles indicate the time steps Δt_n. Panel (b): evolution of the residence time scale. Dashed line shows length of output interval (3600 s). Output interval Δt_s also indicated in time as vertical lines. Panels (c) and (d): detailed view of panels (a) and (b), respectively, during the storm peak.

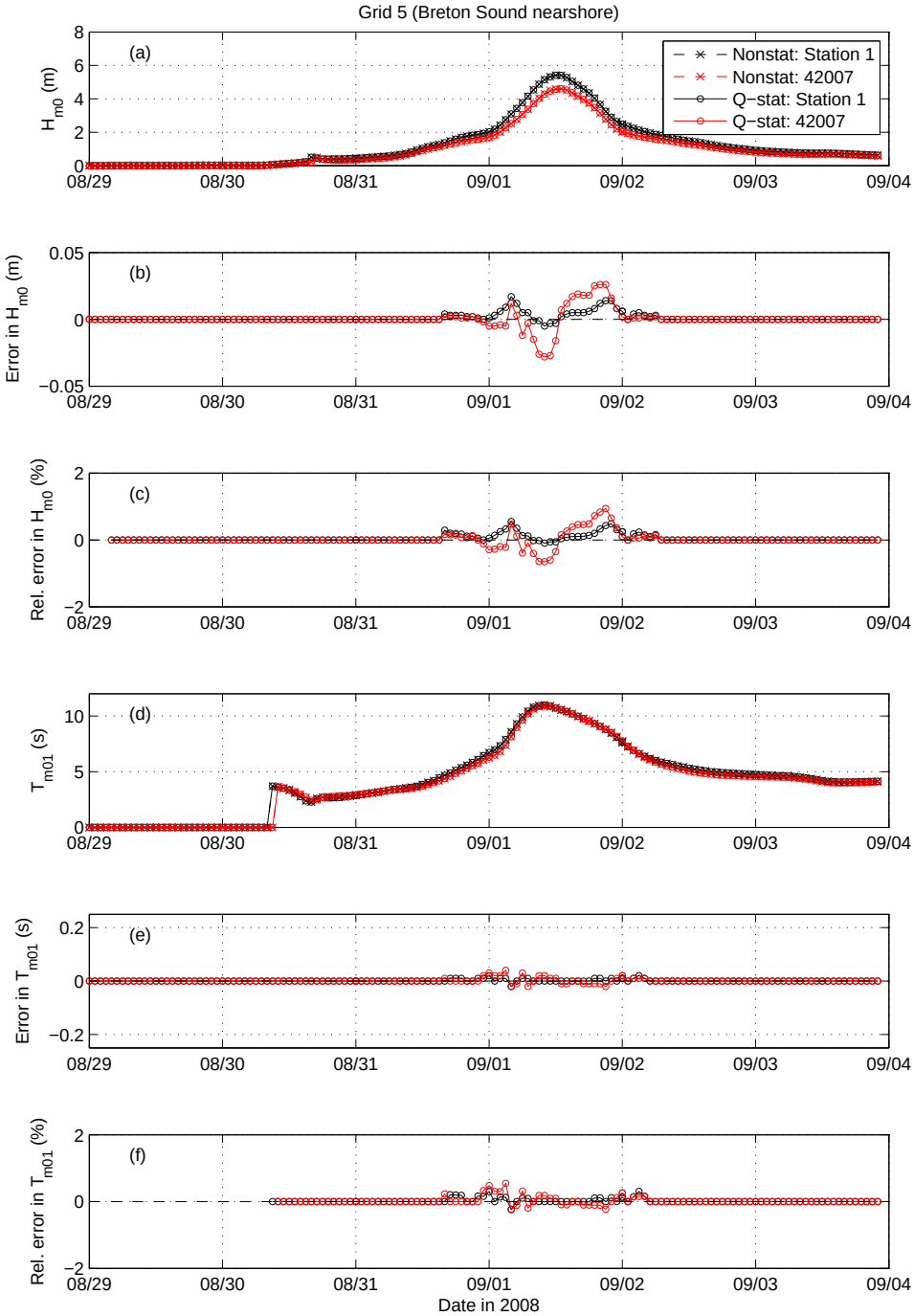

Fig. 7: Comparison between quasi-stationary and default nonstationary model results for Hurricane Gustav case on Grid 5 at output intervals Δt_s. Panel (a): evolution of H_{m0} at two stations. Panel (b): difference in H_{m0} result between quasi-stationary and nonstationary models. Panel (c) percentage difference in H_{m0} result between quasi-stationary and nonstationary models. Panels (d)–(f): as in panels (a)–(c), but for the mean period T_{m01}.

4 DISCUSSION

In the present study, a quasi-stationary version of WW3 was developed, based on explicit hyperbolic equations for spatial propagation. This approach takes advantage of the fact that over a nearshore domain of limited extent, the residence time of wave energy t_s may be shorter than the output time step used in the model Δt_s. The simulation can therefore, in principle, be sped up by a factor equal to the ratio $\Delta t_s/t_s$ designated here by γ. This speeding-up depends on the wave conditions, as γ depends on t_s, and therefore the wave energy propagation speed (i.e. frequency), and also on grid extent and orientation. For example, in the idealized propagation case (Section 3) the speed-up gradually reduced during the simulation due to the effect of dispersion on the spectral components arriving from offshore. In the hurricane field case, the mean frequency, and hence model speed-up is connected to the hurricane wind structure, and hence varied with the location of the hurricane relative to the nearshore quasi-stationary domain.

From the above it would seem logical to apply a variable γ in the quasi-stationary model mode. However, greater gains in computational speed may be had by applying a fixed γ of greater magnitude. Also, in an operational setting such as that at the National Centers for Environmental Prediction (NCEP), a varying γ, and hence varying simulation time may be problematic, since it is desirable to have predicable, fixed simulation times in this context. One approach could be to select a fixed t_s (and hence γ) based on typical wave conditions over a specific coastal region. Since the actual residence time of the wave field will vary between events, a constant t_s may, however, frequently be an underestimation of this actual residence time during a given simulation period. This implies that the error with respect to the default nonstationary solution would also vary during the simulation. This is illustrated in Figures 8 and 9, where the Hurricane Gustav case is run with a constant t_s set to 1800 s, the value reached during the peak of the event, during which $T_{\mathrm{m01}} \approx 10$ s. This setting implies a fixed computational time saving of approximately 50% relative to the default nonstationary model (from 67 min to 34 min). It can be seen that away from the peak of the event, where the wave field is younger, the errors with respect to the default nonstationary simulation become larger than with the adaptive t_s (compare Figures 7 and 9). As may be expected, the errors mainly take the form of a phase lag with respect to the default nonstationary result, underestimating wave heights during periods of increasing H_{m0}, and overestimating them during periods of reducing values (Figure 9(b)). Considering the results in terms of relative error (Figures 9(c) and (f)), the errors in the energetic period of the event (08/31–09/04) remain below 5% and 2% for H_{m0} and T_{m01} respectively. However, closer to the peak of the event, where the most important model results are arguably found from an application point of view, the errors remain much smaller than this, since here the constant t_s agrees better with the actual residence time of the wave condition. It would therefore be possible to select a constant t_s (based on the mean wave climate) that would act as a filter: wave conditions of this maturity level and higher would be represented with minimal error relative to the fully nonstationary solution, whereas less mature wave fields (with greater residence times) would be reproduced with a larger, but accepted, margin of error. A conservative approach would clearly be to set the time scale t_s at a high value (>1800 s in this example) to minimize this error, but this choice must be weighed up the increase in computational cost.

Although, as discussed above, the speed of nearshore simulation can be enhanced by increasing the factor γ, the computational effort will inevitably increase due to the CFL time step constraint inherent in explicit propagation schemes. Assuming that the CFL number is to remain equal moving from the offshore to the nearshore, the required reduction in the nearshore propagation time step was estimated as the ratio of the nearshore to offshore resolutions β in Section 2. The total impact on the effective time step relative to nonstationary simulations in the offshore is therefore given by $\gamma\beta$. The highest grid resolution currently run operationally at NCEP is 4 arc-min, over shelf regions. For the Hurricane Gustav simulation, for example, the nearshore quasi-stationary nested Grid 5 had a resolution of 100 m (Table 1). The ratio of the latter and the 4 arc-min NCEP grid yields $\beta = 0.013$, so that with a constant $\gamma = 2$, we have $\gamma\beta \approx 0.03$. Inserting this into (13), it can be seen that despite the speed-up afforded by quasi-stationary simulation, nearshore simulation using explicit propagation schemes still represents a significant reduction in the effective time step relative to offshore simulations, and therefore an increase in total computational time.

The question therefore arises as to how the present quasi-stationary approach relates to the stationary, implicit scheme approaches available in models such

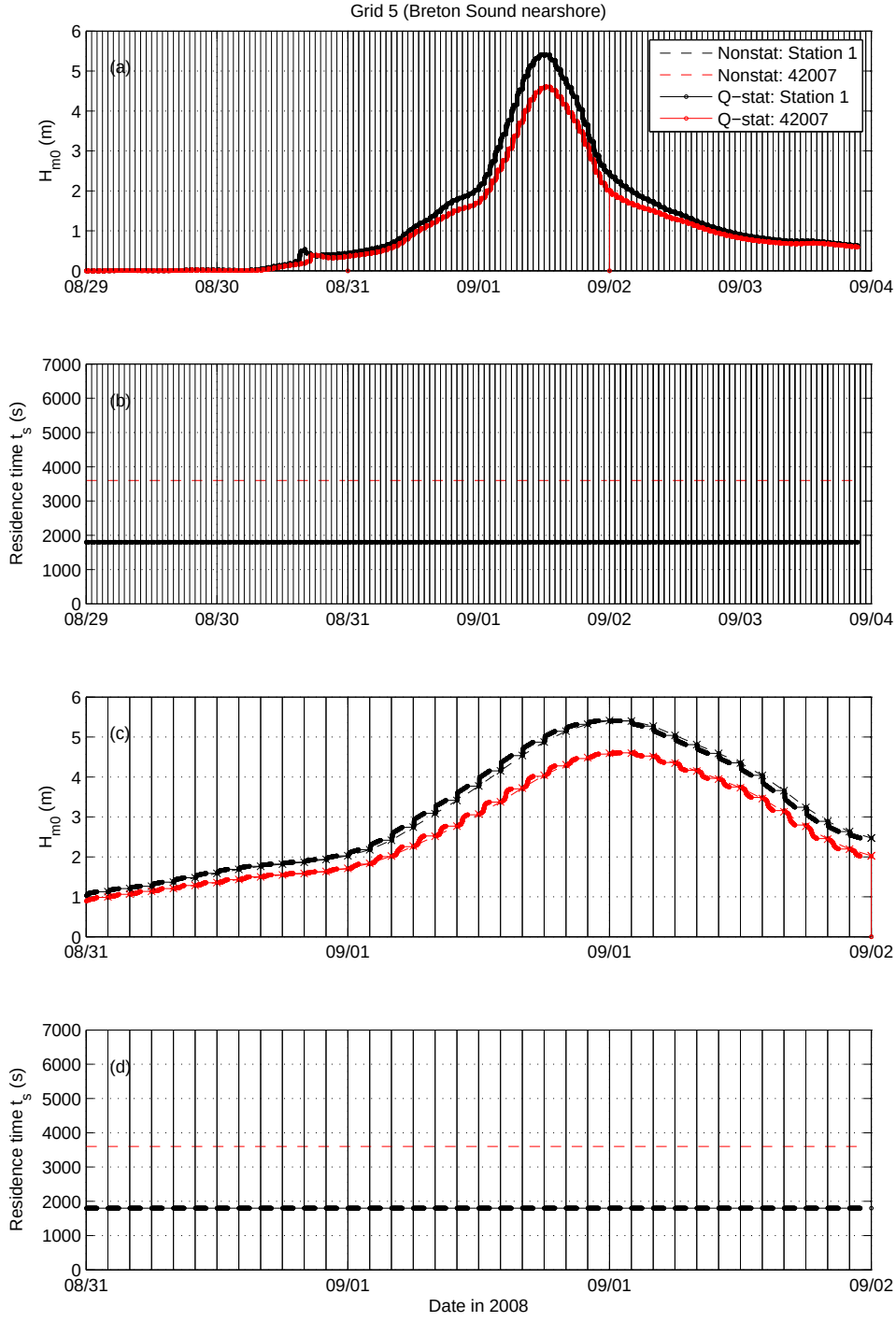

Fig. 8: As in Figure 6, but for a constant, imposed residence time of $t_s = 1800$ s.

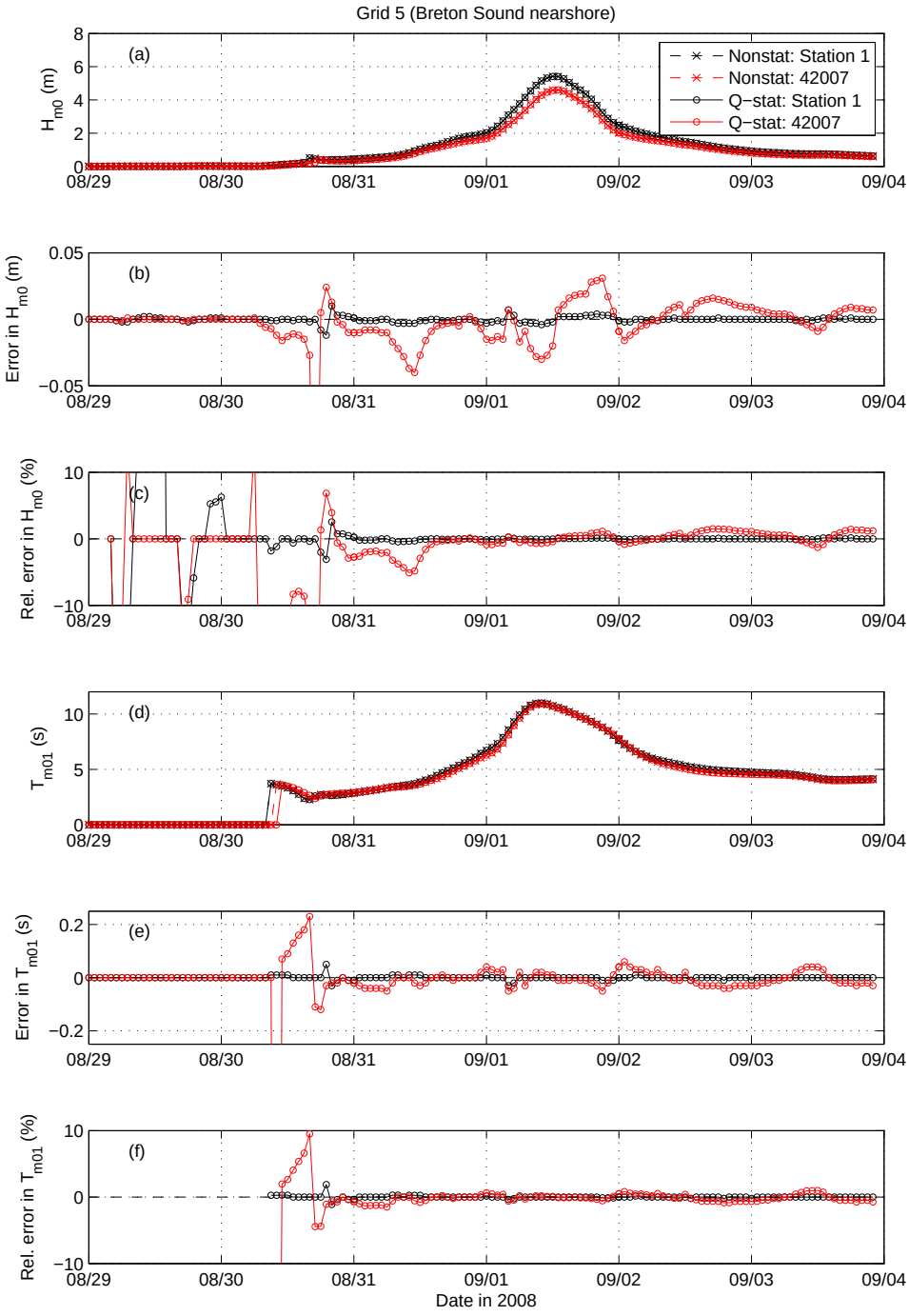

Fig. 9: As in Figure 7, but for a constant, imposed residence time of $t_s = 1800$ s.

as SWAN. The quasi-stationary approach provides a natural extension of the fully nonstationary mode of WW3 in the nearshore. The parameter γ can be used to differentiate between nonstationary ($\gamma < 1$) and (quasi-) stationary ($\gamma > 1$) conditions, enabeling a smooth transition within the same WW3 simulation, as shown in Section 3. It adheres to the CFL criterion, and hence results in very little error (e.g. due to diffusion) relative to the original nonstationary solution. As shown above, the level of error incurred in the quasi-stationary model can in fact be quantified in terms of the residence time, and hence be optimized. Implicit scheme, stationary approaches do not share these benefits. Stationarity is assumed *a priori*, and the elliptical propagation schemes transport wave information to the coast instantly, resulting in a negative phase lag in swell propagation. Also, the error relative to the original nonstationary solution cannot be controlled, so that the loss in accuracy and the computational speed-up cannot be balanced. Note that the stationary elliptical scheme typically requires iterative solution because of nonlinearities and wave refraction (Zijlema and Van der Westhuysen, 2005). This can be considered as being analogous to time stepping with an explicit scheme, although it is expected to be cheaper.

Finally, we turn to the question of quasi-stationary operation in the context of the multi-grid (mosaic) version of WW3. All simulations presented in this study were run in a one-way nested manner, with information going exclusively from the offshore to the nearshore nested domain. Considering the limited scale of the domains for quasi-stationary simulation, and the typical orientation of the information flow, this may often be sufficient from a physical point of view. However, in some cases, information may also flow from nearshore domains back to the offshore, for example with offshore winds or in the vicinity of barrier islands, so that inclusion of the quasi-stationary approach in ww3_multi should be considered. This extension would be relatively straight-forward. In the multi-grid system, a nested set of grids, ranging from coarse to fine, is assigned corresponding ranks, from low to high (Tolman, 2007). The various grids need to be synchronized on a regular basis in order to maintain numerical accuracy. For simplicity, a single global synchronization time t_{sync} is applied. This is computed as the smaller of the input/output interval Δt_s and the smallest Δt_n of the grid with the lowest rank number (outermost coarse grid). In a quasi-stationary context, if Δt_n of the lowest ranked grid would be smaller than the input/output interval Δt_s, synchronization would occur within one Δt_s cycle of the quasi-stationary run. This would pose a problem for the quasi-stationary approach, which, within the unit of the Δt_s cycle, requires boundary conditions (from an equal or lower rank) that are $(\Delta t_s - t_s)$ ahead of the current time step t_i. Hence, synchronization between the quasi-stationary domain and the remaining ranks would only be possible once every input/output cycle Δt_s.

In order not to disrupt the global algorithm of the current multi-grid system, a reasonable methodology therefore appears to be to maintain the present computation of t_{sync} (minimum of Δt_s and Δt_n on the lowest rank), but to synchronize with the quasi-stationary domain(s) only every Δt_s. Considering again the typical information flow from offshore to the nearshore, the reduced updating frequency to the quasi-stationary nearshore domain is not expected to result in significant spurious model behavior. This is being pursued in a follow-up study.

5 CONCLUSIONS

In the present study, a quasi-stationary version of WW3 was developed for application to nearshore domains, based on the explicit hyperbolic propagation schemes. The quasi-stationary model version takes advantage of the fact that the residence time of wave energy becomes short over limited nearshore domains, leading to quasi-stationary conditions. This can be used to reduce simulation times over these domains by means of a time stretching principle. This principle was worked out and evaluated for an idealized propagation case and a highly nonstationary hurricane field case. The following conclusions can be drawn from the results of this study:

1. In the nearshore, the requirement for smaller spatial steps leads to a reduction of the CFL time step associated with explicit schemes for spatial propagation of wave energy. The resulting increase in computational effort can be partially offset by the quasi-stationary approach proposed in this study, by taking into account the difference between the interval for model input/output Δt_s and the propagation time of wave energy through the nearshore domain (residence time, t_s). When expressing the ratio of these two time scales as γ, quasi-stationary operation is possible for $\gamma > 1$.

2. Quasi-stationary operation (i.e. $\gamma > 1$) is found to be possible for an idealized propagation case and a field case with highly non-

stationary hurricane wind forcing. In the field cases considered here, quasi-stationary operation is found to yield up to 50% reduction in computational time locally with respect to fully nonstationary simulation in the nearshore. However, taken over the entire simulation time, the run time came to 91% of that of the default nonstationary model. This speed-up is, however, dependent on the wave conditions and quasi-stationary grid extent. For the cases considered, maximum errors in H_{m0} and T_{m01} with respect to the nonstationary model results were found to be only 1% and 0.5%, respectively.

3. Further savings were shown to be achievable by applying a constant residence time scale of $\gamma = 2$, say. This implies a saving relative to nonstationary model runs of about 50%. In the single field case considered, this increased the error in H_{m0} and T_{m01} to 5% and 2%, respectively, which is considered to be acceptable.

4. When expressing the ratio of the nearshore to offshore grid cell sizes as β (< 1), the resulting impact on the effective propagation time step going from offshore to nearshore can be expressed as a factor $\gamma\beta$. Even though the quasi-stationary time scale γ was often found to be greater than one in the cases considered here, the product $\gamma\beta$ is expected to typically be smaller than one. This implies a significant increase in simulation time in the nearshore compared to domains of similar total grid point size in the offshore.

6 ACKNOWLEDGMENTS

The authors would like to thank Erick Rogers, Aron Roland, Arun Chawla and Roberto Padilla for useful discussions on this work. Jim Chen and Arun Chawla are thanked for providing the data and computational grids for the Hurricane Gustav field case.

References

Booij, N., R. C. Ris and L. H. Holthuijsen, 1999: A third-generation wave model for coastal regions, Part I, Model description and validation. *J. Geophys. Res.*, **104**, 7649–7666.

Brown, J. M. and J. Wolf, 2009: Coupled wave and surge modelling for the eastern Irish Sea and implications for model wind-stress. *Continental Shelf Research*, **29(10)**, 1329–1342, doi: 10.1016/j.cr.2009.03.004.

Chen, Q., K. Hu and A. Kennedy, 2010: Numerical modeling of observed hurricane waves in deep and shallow waters. *Proc. 32th Int. Conf. Coastal Eng., ASCE*.

Davis, J. E., 1992: STWAVE theory and program documentation, Coastal Modeling System User's Manual. Instruction Report CERC-91-1, Supplement 1, U.S. Army Engineer Waterways Experiment Station, Vicksburg, MS.

Hasselmann, K., 1960: Grundgleichungen der seegangsvoraussage (in german). *Schiffstechnik*, **1**, 191–195.

Holthuijsen, L. H., N. Booij and T. H. C. Herbers, 1989: A prediction model for stationary, short-crested waves in shallow water with ambient currents. *Coastal Engineering*, **13**, 23–54.

Hu, K., Q. Chen and S. K. Kimball, 2010: Consistency in hurricane surface wind forecasting: An improved parametric model. *Submitted*.

Luettich, Jr., R. A. and J. J. Westerink, 2004: Formulation and numerical implementation of the 2D/3D ADCIRC Finite Element Model Version 44.xx. Tech. Rep. http://adcirc.org/adcirc_theory_2004_12_08.pdf2004.

Monbaliu, J., R. Padilla-Hernandez, J. Hargreaves, J. Albiach, W. Luo, M. Sclavo and H. Gunther, 2000: The spectral wave model, WAM, adapted for applications with high spatial resolution. *Coastal Engineering*, **41(1-3)**, 41–62. doi:10.1016/S0378–3839(00)00026–0.

National Hurricane Center, 2008: Tropical Cyclone Report Hurricane Gustav (AL072008). Tech. Rep. www.nhc.noaa.gov/pdf/TCR-AL072008_Gustav.pdf.

Smith, J. M., D. T. Resio and A. K. Zundel, 1999: STWAVE: Steady-state spectral wave model; Report 1: Users manual for STWAVE version 2.0. Instructional Report CHL-99-1, U.S. Army Engineer Waterways Experiment Station, Vicksburg, MS.

Tolman, H. L., 2007: Development of a multi-grid version of WAVEWATCH III. Tech. Note 256, NOAA/NWS/NCEP/MMAB, 88 pp. + Appendices.

Tolman, H. L., 2009: User manual and system documentation of WAVEWATCH III ^{TM} version 3.14. Tech. Note 276, NOAA/NWS/NCEP/MMAB, 194 pp. + Appendices.

Tolman, H. L., 2010: A note on stationary wave modeling with WAVEWATCH III ^{TM}. Tech. Note 287, NOAA/NWS/NCEP/MMAB, 5 pp.

Tolman, H. L. and D. V. Chalikov, 1996: Source terms in a third-generation wind-wave model. *J. Phys. Oceanogr.*, **26**, 2497–2518.

Westerink, J. J., R. A. Luettich, Jr., J. C. Feyen, J. H. Atkinson, C. Dawson, M. D. Powell, J. P. Dunion, H. J. Roberts, E. J. Kubatko and H. Pourtaheri, 2008: A basin to channel scale unstructured grid hurricane storm surge sodel as implemented for Southern Louisiana. *Monthly Weather Review*, **136**, 833–864.

Zijlema, M. and A. J. van der Westhuysen, 2005: On convergence behaviour and numerical accuracy in stationary SWAN simulation of nearshore wave spectra. *Coastal Engineering*, **52**, 237–256.